# Fully flexible temporal resolution for energy system optimization

Gao, Zhi; Gazzani, Matteo; Tejada-Arango, Diego A.; Soares Siqueira, Abel; Wang, Ni; Gibescu, Madeleine; Morales-España, Germán

**DOI**
10.1016/j.apenergy.2025.126267

**Publication date**
2025

**Document Version**
Final published version

**Published in**
Applied Energy

**Citation (APA)**
Gao, Z., Gazzani, M., Tejada-Arango, D. A., Soares Siqueira, A., Wang, N., Gibescu, M., & Morales-España, G. (2025). Fully flexible temporal resolution for energy system optimization. *Applied Energy*, *396*, Article 126267. https://doi.org/10.1016/j.apenergy.2025.126267

Applied Energy 396 (2025) 126267

Contents lists available at ScienceDirect

Applied Energy

journal homepage: www.elsevier.com/locate/apen

# Fully flexible temporal resolution for energy system optimization

Zhi Gao [a], Matteo Gazzani [a,b,*], Diego A. Tejada-Arango [c,d], Abel Soares Siqueira [e], Ni Wang [c], Madeleine Gibescu [a], Germán Morales-España [c,f]

[a] Copernicus Institute of Sustainable Development, Utrecht University, Utrecht, 3584CS, the Netherlands
[b] Sustainable Process Engineering, Chemical Engineering and Chemistry, Eindhoven University of Technology, Eindhoven, 5612 AP, the Netherlands
[c] TNO Energy Transition, Amsterdam, the Netherlands
[d] Instituto de Investigación Tecnológica, Escuela Técnica Superior de Ingeniería, Universidad Pontificia Comillas, Madrid, Spain
[e] Netherlands eScience Center, Amsterdam, the Netherlands
[f] Faculty of Electrical Engineering, Mathematics and Computer Science, Delft University of Technology, Delft, the Netherlands

## HIGHLIGHTS

- Fully flexible formulation for temporal aggregation in energy system models.
- Flexible temporal resolution preserves the laws of Physics.
- Computing algorithms provided for easy implementation.
- The time formulation allows for improvements in computational efficiency.

## GRAPHICAL ABSTRACT

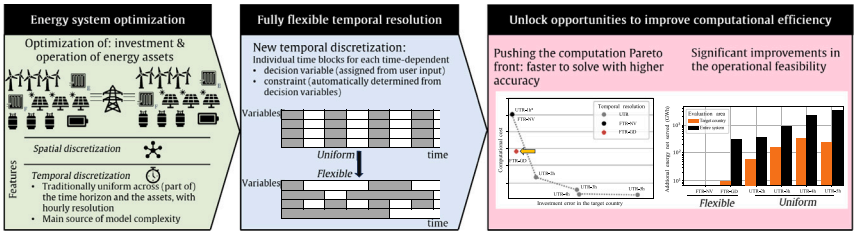


## ARTICLE INFO

*Keywords:*
Energy system optimization
Temporal aggregation
Computational efficiency

## ABSTRACT

In order to achieve a timely transition towards sustainable energy systems within a large landscape of multi-sectors and multi-technologies, decision-makers and industry practitioners can rely on time- and space-discretized energy system optimization models. However, such models are often burdened by the computational costs arising from the growing problem complexity, which is especially due to the time discretization. The common strategy to lower the computational cost is to uniformly reduce the temporal resolution, sacrificing the quality of the solution. In light of this, we propose the concept and a formulation of fully flexible temporal resolution, wherein each decision variable and constraint can have a separate temporal resolution. After introducing the formulation in detail, we demonstrate its capability by applying it to an EU-wide case study optimizing both capacity investment and operation decisions of the inter-connected energy system across the different countries. We show that the proposed flexible formulation allows us to flexibly remove variables and constraints that are not needed without losing accuracy, and to simplify the time discretization (e.g., in space) while pushing the Pareto front by simultaneously speeding up computation and limiting losses in accuracy. In conclusion, we highlight the promise of adopting fully flexible temporal resolution and encourage future research to explore further temporal resolution configurations beyond our examples.

## 1. Introduction

Under the ambition of timely reaching a net-zero $CO_2$ society, most of the world's economies are taking urgent actions to transform their energy systems to reduce Greenhouse Gas (GHG) emissions [2,3]. In order to navigate this complex transformation, many actors rely on Energy System Optimization Models (ESOMs), from decision-makers

* Corresponding author at: Copernicus Institute of Sustainable Development, Utrecht University, Utrecht, 3584CS, the Netherlands
*Email address:* m.gazzani@uu.nl;gazzanim@ethz.ch (M. Gazzani).

https://doi.org/10.1016/j.apenergy.2025.126267
Received 11 April 2025; Received in revised form 28 May 2025; Accepted 31 May 2025
Available online 17 June 2025

**Nomenclature**

*Sets*

| | |
|---|---|
| $V(c)$ | Decision variables in constraint $c$ |
| $\mathcal{A}$ | Energy assets |
| $\mathcal{A}^{\text{invest}}$ | Assets that can be invested in |
| $\mathcal{A}^{\text{conversion}}$ | Conversion assets |
| $\mathcal{A}^{\text{storage}}$ | Storage assets |
| $\mathcal{A}^{\text{producer}}$ | Producer assets |
| $\mathcal{F}$ | Energy flow connections |
| $\mathcal{F}^{\text{invest}}$ | Investable flow connections |
| $\mathcal{F}^{\text{in}}$ | Arriving flow connections |
| $\mathcal{F}^{\text{out}}$ | Leaving flow connections |

*Decision variables*

| | |
|---|---|
| $v$ | General decision variables |
| $v^{\text{invest}}$ | Invested capacity |
| $v^{\text{flow}}$ | Energy flow rate (The energy flow rate decision variables represent energy flow rates (e.g., in MW). The energy content is obtained by multiplying $v^{\text{flow}}$ with the corresponding duration $\ell$) |
| $v^{\text{charging}}$ | Charging state |
| $v^{\text{stored}}$ | Stored energy |
| $v^{\text{inflow}}$ | Extra energy inflow |

*Parameters*

| | |
|---|---|
| $p$ | General parameters |
| $p^{\text{invest\_cost}}$ | Capacity investment cost |
| $p^{\text{variable\_cost}}$ | Variable operational cost |
| $p^{\text{invest\_limit}}$ | Investment limit |
| $p^{\text{availability\_profile}}$ | Availability profile |
| $p^{\text{energy\_to\_power\_ratio}}$ | Energy-to-power ratio |
| $p^{\text{efficiency}}$ | Efficiency |
| $p^{\text{demand\_profile}}$ | Demand profile |
| $p^{\text{inflow}}$ | Available extra energy inflow |

*Other symbols*

| | |
|---|---|
| $u$ | Base unit period length |
| $T$ | Horizon length |
| $\mathcal{R}$ | Resolution containing time blocks (In Tulipa energy model [1], "partition" is used instead to denote temporal resolutions) |
| $b$ | Time block |
| $i, j$ | Indices of time blocks |
| $s$ | Time block starting time |
| $e$ | Time block ending time |
| $\ell$ | Duration of time block |
| $\ell^{c,v}_{j,i}$ | Map of duration between decision variable $v$ and constraint $c$ |

in governmental institutions to practitioners in private companies. An ESOM requires to have a bottom-up mathematical representation of the energy system's physical nature. This includes discretizing the temporal horizon, segmenting the energy network geographically, and providing detailed descriptions of energy technologies, among other factors [4]. The outcome of ESOMs often encompasses the optimal system design and its transitional path, operational decisions and marginal commodity prices under user-defined scenarios [5]. Like with other computer models, ESOM designers face the trade-off between solution accuracy and computation capacity [6]. Having a more intricate representation of the problem frequently leads to higher computation costs. In fact, under the limitations of conventional computation power – few industrial practitioners or policy-makers have broad access to supercomputing facilities –, most large problems are not yet solvable at the desired level of detail [7,8].

Still, the complexity of energy systems inevitably increases with the emergence of non-traditional energy technologies, such as intermittent renewable energy generators and distributed energy storage, as well as the coupling of multiple energy sectors like electricity, heat and hydrogen [9,10]. Within this context, the interconnection of energy assets and energy systems has taken an even more important role for the optimal decision-making in capacity investment and operation: energy networks need to be adequately represented in ESOMs in order to draw meaningful conclusions [11,12]. As a result, the problems that ESOMs aim to address are becoming more complex. Consequently, it has become an even more pressing challenge to push the accuracy–computation Pareto front: Whether we can enhance the problem accuracy without significantly increasing the computational cost and whether we can build less expensive ESOMs without compromising the solution quality, as for example demonstrated in [13,14].

One can think of complex energy systems optimization as planning an orchestra performance. The orchestra conductor (optimization algorithm) must decide what, when, and how each instrument (conversion, storage, and transport technologies) plays to create a harmonious performance (optimal costs or minimum emissions). Just like in energy system optimization, the conductor must make optimal choices within given constraints – the musical pentagram in music, or the physical laws and system limits in energy systems – to achieve the optimal outcome. To simplify the complex task of a conductor, unnecessary adjustments can be removed when not needed, and certain instruments can be limited to specific sequences in a symphony (after all, a continuous gong might not be so harmonious). The approach we present in this work follows a similar logic applied to energy system optimization: allowing for flexible adjustment of time discretization per physical element in the system to retain decision moments when needed, while eliminating or aggregating periods that have minimal impact on the optimal solution.

In fact, probably not surprisingly, among the elements of the mathematical representation in ESOMs, temporal resolution has been identified as the primary driver of the problem size [15]. This is because, in the typical formulation of ESOMs, operational variables are coupled to every time step. Additional challenges arise when looking at storage technologies. This means that the number of variables and the associated constraints is directly proportional to the total number of time steps within the problem horizon. On the other hand, the number of time steps surpasses the count of geographical nodes and technological specifics by orders of magnitude, especially in multi-year problems [16]. Consequently, improving or simplifying the temporal representation holds considerable potential for tackling the accuracy–computation Pareto front. And opportunities lie in the two aforementioned factors, reducing the number of time steps and making the temporal resolution of operational variables flexible.

In the literature, substantial efforts have been directed towards reducing the number of time steps, as evident from the literature reviews in [16,17]. One straightforward way is to decrease the hourly temporal resolution of the entire system. For instance, Shirizadeh and Quirion [18] investigated the effects of setting time steps every 2, 4 and 8 h in an ESOM of a multi-carrier energy system. Despite the cut in calculation time, ineligible errors occur and are pronounced further when the system is dominated by wind and solar energy. Notably, Weimann and Gazzani [13] exploited the regular underestimation of technology capacities when employing a reduced temporal resolution. They proposed a simplification method that sets the solution for its temporally coarser counterpart problem as the minimum installed technology capacity in the finer problem. While this method facilitates the usage of hourly time

series, it is infeasible when dealing with competing technologies (e.g., two similar types of wind or gas turbines) due to the minimum capacity constraints.

Another popular approach is using representative periods instead of the sequential time horizon. When representative periods are treated independently from each other, though the short-term system dynamics within the representative periods are captured, compatibility with long-term dynamic features such as energy storage is compromised [19]. To address this challenge, methods have been devised to link the representative periods to the long-term horizon, which enables the participation of long-term storage and, therefore, considerably improves the solution accuracy [20,21]. Nonetheless, errors are inevitable because of the statistical inaccuracies in time-series aggregation and their nonlinear relationship with optimization solutions [16].

Yet, exploring flexibility in the temporal resolution remains uncommon. The majority of ESOMs construct the energy system using a uniform temporal resolution across the system or by each sector [22–27]. Specifically, operational variables for all energy technologies at all nodes, along with constraints, such as instantaneous energy balances for all energy carriers and energy storage logic, are established for each time step. As an exception, in the case of Ihlemann et al. [28], the user can customize the temporal resolution of specific parts of the energy system. However, the resolutions are still not fully independent, as period lengths need to be in multiples of each other to generate the constraints correctly.

For single-carrier ESOMs, having non-uniform temporal resolutions for different technologies can shorten the computation time with limited errors. A reason is that, even when using the same energy carrier, energy technologies can function on various timescales: like a gong in an orchestra, an open cycle gas turbine is used selectively only to cover demand peaks. As an example, Renaldi et al. [29] show such benefits when they assign a lower temporal resolution to long-term thermal storage units, while other storage units remain in their original resolution. Furthermore, even for the same technology, its operations can have a certain (predictable) pattern over the time horizon. For instance, the production of solar energy during the night is always zero, and therefore it should not deserve the same resolution as periods during the day. A more intricate example is the seasonal thermal demand. In the summer, the demand for cooling is likely to be more resonant and varying than that in the winter, and vice versa for the electric heating demand [30]. It would be more efficient to spend the computational resources dynamically in the time horizon of ESOMs.

For multi-carrier ESOMs, it is self-evident that each energy sector should have its own temporal resolution, owing to their distinct physical characteristics and time constants governing their dynamics. Let's consider the integration of electricity and hydrogen sectors as an example. For the electricity sector, an hourly resolution is considered sufficient to capture the intermittency of variable renewable energy sources, given that the influences of weather phenomena (e.g., wind speed and solar irradiation) within the one-hour time-frame tend to cancel each other out at system scale [31]. Although sub-hourly resolution could better represent the flexibility of thermal generation units [32], the hourly resolution is still commonly adopted as a standard approach owing to the computational cost trade-off [33]. By contrast, the hydrogen sector can accommodate a lower temporal resolution. When hydrogen is connected to the electricity sector via processes like electrolysis and reverse electrolysis (via fuel cells), the interaction should indeed adhere to the hourly resolution of the electricity sector. However, when considering the accumulated energy content, hydrogen storage predominantly follows seasonal or even annual working cycles, as demonstrated in [34]. Therefore, there is great potential in modeling hydrogen storage with longer time intervals. In fact, in [35] Martínez-Gordón et al. did set an hourly resolution for the power sector, heat network and cross-sector flexibility options, at the same time modeling the hydrogen and gas sectors with daily resolution. Similarly, Morales-España et al. [36] combine the hydrogen sector in six-hourly resolution with the hourly electricity sector. This kind of adaptive temporal resolution aids in capturing fluctuations in renewable power output and responses in energy storage while maintaining the problem's complexity and computational tractability at a manageable level.

Motivated by the above knowledge gap, we present in this paper the concept, formulation, and implementation of fully flexible temporal resolution. As shown in Fig. 1, the fully flexible temporal resolution relies on user decisions (configuration of time for each decision variable) and on automated algorithms (formulation of the resulting constraints' resolution). Thanks to its flexibility, which provides the user with an additional instrument to simplify the problem without affecting the quality, the formulation can result in an optimization problem that solves faster with a low-to-no-error solution, depending on the temporal resolutions given in the user input. In the analysis of the result, we compare with traditional uniform temporal aggregations, as our formulation is compatible, and not competing with most hourly-based time series aggregation methods, such as the aforementioned representative periods. The three main contributions of this work can be summarized as follows:

- We introduce the concept and provide the mathematical formulation of *fully flexible* temporal resolutions, wherein not only does each time-coupled decision variable or constraint possess its distinct time blocks representing different durations, but also they do not need to be multiples of each other.
- We examine the inter-dependencies of the fully flexible temporal resolution and formulate requirements to abide by the physical laws pertaining to each modeled technology. We also provide computational algorithms to determine the temporal resolutions that satisfy these requirements.
- We implement the concept, mathematical formulation and algorithms in a large-scale case study of the European energy system. We demonstrate significant improvements in computational efficiency and solution accuracy, achievable through a few temporal resolution configurations enabled by our formulation.

The remainder of this paper is structured as follows. In Section 2 we present the concept of fully flexible temporal resolution with a concise yet explicit example, and we outline the necessary determination of temporal resolution to construct the constraints respecting the physics they are representing, with supporting algorithms. In Section 3, we reformulate an energy system optimization problem accordingly. Section 4 details the application of our formulation to a case study of the energy systems in 27 EU countries plus the UK, Norway and Switzerland. In Section 5, we show the results and discuss the effects of temporal resolution configurations enabled by our formulation, followed by conclusions in Section 6.

## 2. Fully flexible temporal resolution

### 2.1. Concept

The concept underlying the mathematical formulation of the fully flexible temporal resolution is distinguished by the following features:

1. Each time-dependent decision variable and constraint has a separate temporal resolution consisting of time blocks.
2. The time blocks can represent different durations that are not necessarily multiples of each other.

To measure the different durations, we require a minimum *base unit* period length $u$, which can be any real time interval length as the modeler sees fit, such as one hour or one day. The time blocks are then represented as multiples of the base unit period length. The length of the horizon $T$ is also given in the total number of base unit periods.

To elaborate further, we show an example of four series of time-dependent decision variables, parameters and constraints in Fig. 2. Traditionally, ESOMs rely on a uniform temporal resolution, as in Fig. 2a, where the decision variables $v_t^1$, $v_t^2$, parameters $p_t$ and constraints

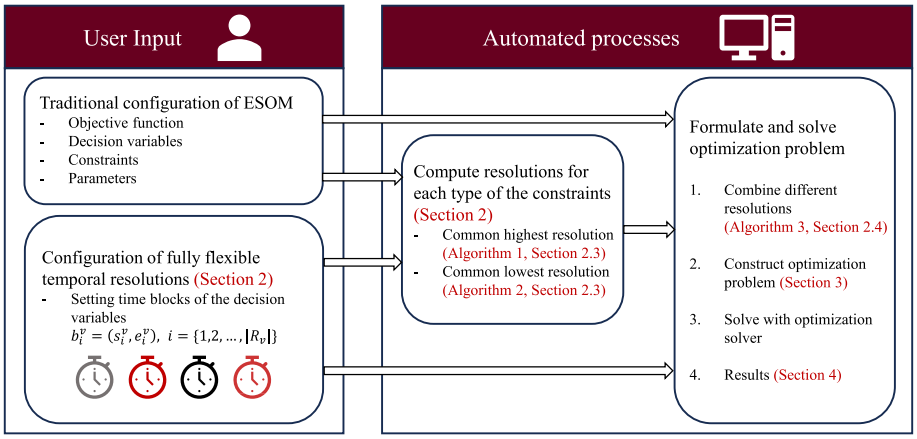


**Fig. 1.** Overview of the energy system optimization model when including the fully flexible temporal resolution, with highlight on the user input and automated processing phases.

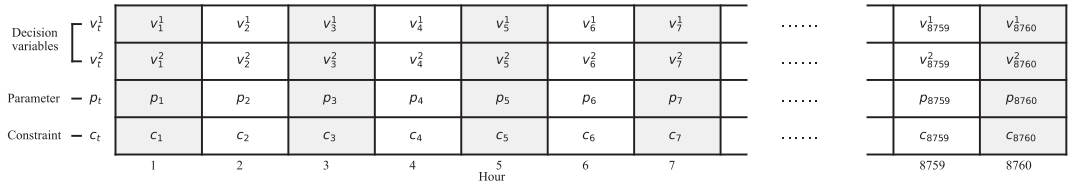


(a) Traditional uniform temporal resolution of decision variable, parameter and constraint series.

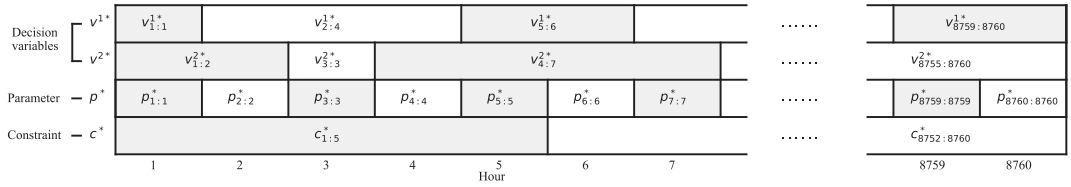


(b) Fully flexible temporal resolution. The decision variable, parameter and constraint series each has a separate resolution.

**Fig. 2.** Example of uniform and fully flexible temporal resolutions.

$c_t$ share, e.g., an hourly resolution with the uniform time index $t$ going from 1 to 8760 of a yearly horizon, ($T = 8760$ h of 365 days, $u = 1$ hour). Whereas applying the fully flexible temporal resolution concept, they can each possess a varying series of time blocks. Fig. 2b demonstrates a possible setup of their temporal resolutions. Decision variables $v^{1*}$, $v^{2*}$, parameter $p^*$ and constraint $c^*$ are series with the fully flexible temporal resolution. The time blocks are no longer of the same length. Note that from here on, we adopt an indexing system that gives the starting and ending time, separated by a colon to designate clearly the temporal position of each time block. The time values are in the number of the unit period, here, an hour. For instance, $v^{1*}_{2:4}$ denotes the variable in $v^{1*}$ series that spans from hour 2 up to and including hour 4.

For a better understanding, let us consider an example of an instantaneous energy balance at a hub, where the decision variables $v^1$ and $v^2$ represent non-negative energy flow rates (e.g., in MW) arriving and leaving the hub, respectively, which are constant during their time block. Parameter $p$ is the consumer demand. Constraint $c$ denotes the energy balance constraint, i.e., The net energy flow at the hub is equal to the demand for every period of the energy balance. We limit the example to the first 5 h, as the constraints are fully displayed in both Figs. 2a and 2b. In the traditional uniform resolution example, we have

$$v_1^1 - v_1^2 = p_1 \quad (c_1) \tag{1}$$
$$v_2^1 - v_2^2 = p_2 \quad (c_2) \tag{2}$$
$$v_3^1 - v_3^2 = p_3 \quad (c_3) \tag{3}$$
$$v_4^1 - v_4^2 = p_4 \quad (c_4) \tag{4}$$
$$v_5^1 - v_5^2 = p_5 \quad (c_5) \tag{5}$$

When we apply the fully flexible temporal resolution, the constraints will be different, depending on the resolution setup. In the example following the resolution of the constraint in Fig. 2b, we have for the first 5 periods–noting again that decision variables $v^{1*}$ and $v^{2*}$ represent energy flow rates which are considered constant within their respective time blocks:

$$\begin{aligned}&(v^{1*}_{1:1} + 3v^{1*}_{2:4} + v^{1*}_{5:6}) - (2v^{2*}_{1:2} + v^{2*}_{3:3} + 2v^{2*}_{4:7})\\ &\quad = (p^*_{1:1} + p^*_{2:2} + p^*_{3:3} + p^*_{4:4} + p^*_{5:5}) \quad (c^*_{1:5})\end{aligned} \tag{6}$$

The constraint now includes pertinent decision variables and parameters, timed by their length of time period in the constraint to balance the energy content. Later, we will show how this constraint can be written in different ways depending on the resolution of the decision variables, and the purpose of the constraint, which also determines the resolution of the constraint.

### 2.2. Selecting the temporal resolutions for constraints

In this new concept, temporal resolutions must be decided differently among time-dependent decision variables, parameters and constraints. We briefly discuss the differences below:

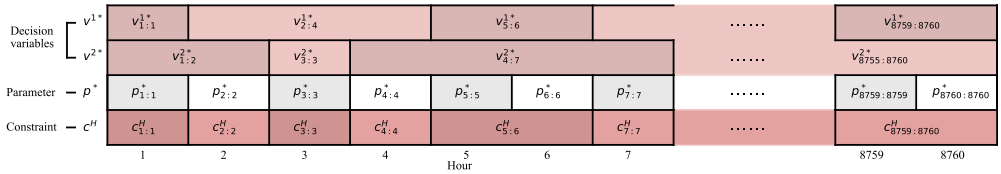


(a) The constraint $C^{\mathrm{H}}$ adopts common highest temporal resolution of the involved decision variables: whenever a new decision variable starts in any of the involved decision variable series, a new time block in the constraint series also starts.

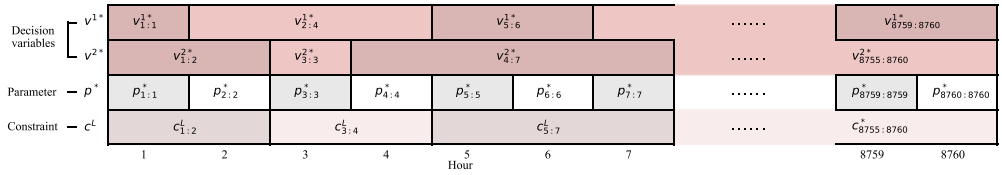


(b) The constraint $C^{\mathrm{L}}$ adopts common lowest temporal resolution of the involved decision variables: setting time blocks of the constraint series to the latest-ending time block of the involved decision variable series.

**Fig. 3.** Common highest and lowest temporal resolution of the involved decision variables.

- Decision variables: their temporal resolutions are defined by the user. Their resolutions directly impact the solution quality, and the user must, based on the requirements, choose the best compromise between computational efficiency and solution accuracy of the energy system optimization problem. Compared to the uniform time discretization, the flexible time resolution introduces an additional tuning opportunity for the user (but also complexity in the input).
- Parameter series: their temporal resolutions are defined by input data. In our formulation later in Section 3, we assume that the parameters are profiled to fit the temporal resolution of the constraint, which can be achieved by using resampling or pre-processing methods if this is not the case.
- Constraint series: it is important that the constraints are formed in a resolution that respects the physical meaning that the constraint represents. Here, we propose algorithms to generate the temporal resolution of the constraints based on the involved decision variables, and we guarantee that the resulting resolution respects the physics that the constraint attempts to model.

Hence, in this section, we identify how the constraints' physical meaning can be distorted or even violated, and discuss the resulting requirements of their temporal resolutions. We categorize the constraints in a general manner, which can be applied to other types of constraints beyond our ESOM in Section 3:

- For constraints based on instantaneous values, usually reflected by the units, e.g. power in MW or MJ/s, at least the common highest temporal resolution of the involved decision variables (Fig. 3a) must be used to guarantee correct modeling, like the examples of instantaneous energy balances and capacity constraints in Sections 2.2.1 and 2.2.2, where the energy flow rate decision variables $v$ or $v^{\mathrm{flow}}$ appear without their durations.
- For constraints based on values that accumulate with time, e.g. energy content in MWh or J, the resolution of the constraint can be obtained by the lowest resolution of the variables involved (Fig. 3b), as in the case of the energy balance of conversion technologies in Section 2.2.3, where the energy flow rate decision variables $v$ or $v^{\mathrm{flow}}$ need to be multiplied with their durations to acquire the energy content.

We provide a more detailed explanation in the following three Sections 2.2.1–2.2.3.

#### 2.2.1. Instantaneous energy balances

Instantaneous energy balances can be violated, when the constraint's temporal resolution does not reach the common highest temporal resolution of the decision variables. Let us first continue with the instantaneous energy balance given in (6), where one feasible solution could be $v^{1*}_{2:4}, v^{1*}_{5:6}, v^{2*}_{1:2}, v^{2*}_{2:3} = 0$, resulting in the following equality:

$$v^{1*}_{1:1} - 2v^{2*}_{4:7} = p^{*}_{1:1} + p^{*}_{2:2} + p^{*}_{3:3} + p^{*}_{4:4} + p^{*}_{5:5} \tag{7}$$

Notice that the energy inflow rate $v^{1*}_{1:1}$ in period 1:1 is providing all the demand for the first 5 periods, including also the outflow rate $v^{2*}_{4:7}$ in period 4:7. That is, this constraint resolution implicitly models storage to respect the energy conservation principle; this fictitious storage effect does not happen in the traditional uniform resolution example in (1)–(5), where the equality balance is imposed at every hour. However, we can completely prevent this undesired fictitious storage effect by writing the constraint in the common highest temporal resolution of the decision variables, as illustrated in Fig. 3a. As specified in Algorithm 1, we obtain this common highest temporal resolution following simple logic: whenever a new decision variable starts in any of the involved decision variable series, a new time block in the constraint series also starts. Now the constraints can be rewritten as

$$v^{1*}_{1:1} - v^{2*}_{1:2} - p^{*}_{1:1} = 0 \quad \left(c^{\mathrm{H}}_{1:1}\right) \tag{8}$$
$$v^{1*}_{2:4} - v^{2*}_{1:2} - p^{*}_{2:2} = 0 \quad \left(c^{\mathrm{H}}_{2:2}\right) \tag{9}$$
$$v^{1*}_{2:4} - v^{2*}_{3:3} - p^{*}_{3:3} = 0 \quad \left(c^{\mathrm{H}}_{3:3}\right) \tag{10}$$
$$v^{1*}_{2:4} - v^{2*}_{4:7} - p^{*}_{4:4} = 0 \quad \left(c^{\mathrm{H}}_{4:4}\right) \tag{11}$$
$$v^{1*}_{5:6} - v^{2*}_{4:7} - \mathrm{mean}\left(p^{*}_{5:5} + p^{*}_{6:6}\right) = 0 \quad \left(c^{\mathrm{H}}_{5:6}\right) \tag{12}$$

With these constraints, the fictitious storage effect exemplified in (7) is no longer possible. In (12), we use the mean value of the hourly demand to keep the energy conservation in the 2-h time block of $c^{\mathrm{H}}_{5:6}$.

#### 2.2.2. Capacity constraints

Another kind of violation can take place in capacity constraints. Let's now consider $v^{1*}$ and $v^{2*}$ as non-negative energy output flow rates, and $p^{*}$ as capacity limit. The capacity limit $p^{*}$ is supposed to set the upper bound of the sum of outputs. If we take the temporal resolutions in Fig. 2b, we will write the capacity constraint as

$$\begin{aligned}&\left(v^{1*}_{1:1} + 3v^{1*}_{2:4} + v^{1*}_{5:6}\right) + \left(2v^{2*}_{1:2} + v^{2*}_{3:3} + 2v^{2*}_{4:7}\right)\\ &\quad \le p^{*}_{1:1} + p^{*}_{2:2} + p^{*}_{3:3} + p^{*}_{4:4} + p^{*}_{5:5} \quad \left(c^{*}_{1:5}\right)\end{aligned} \tag{13}$$

**Algorithm 1** Common highest temporal resolution of involved decision variables in a constraint.

**Input:** Resolution of involved decision variables $\mathcal{R}_v,\ v \in V(c)$
**Output:** Resolution of the constraint $\mathcal{R}_c = \left\{ b_1^c, b_2^c, \dots, b_{|\mathcal{R}_c|}^c \right\}$

```
Initialize an empty list of time blocks for the constraint R_c = [ ]
Initialize the starting time of the time block s* ← 1
while s* ≤ T do
    Define the candidate block end e* ← T
    for v ∈ V(c) do
        Find the time block index i such that s_i^v ≤ s* ≤ e_i^v
        Update the candidate block end if necessary e* ← min(e*, e_i^v)
    end for
    Add the time block (s*, e*) to the end of the list R_c
    Update the starting time for the next block s* ← e* + 1
end while
```

**Algorithm 2** Common lowest temporal resolution of involved decision variables in a constraint.

**Input:** Resolution of involved decision variables $\mathcal{R}_v,\ v \in V(c)$
**Output:** Resolution of the constraint $\mathcal{R}_c = \left\{ b_1^c, b_2^c, \dots, b_{|\mathcal{R}_c|}^c \right\}$

```
Initialize an empty list of time blocks for the constraint R_c = [ ]
Initialize the starting time of the time block s* ← 1
while s* ≤ T do
    Define the candidate block end e* ← s*
    for v ∈ V(c) do
        Find the time block index i such that s_i^v ≤ s* ≤ e_i^v
        Update the candidate block end if necessary e* ← max(e*, e_i^v)
    end for
    Add the time block (s*, e*) to the end of the list R_c
    Update the starting time for the next block s* ← e* + 1
end while
```

Again, one feasible solution could be $v_{1:1}^{1*}, v_{2:4}^{1*}, v_{5:6}^{1*}, v_{1:2}^{2*}, v_{4:7}^{2*} = 0$ and

$$v_{3:3}^{2*} = p_{1:1}^* + p_{2:2}^* + p_{3:3}^* + p_{4:4}^* + p_{5:5}^* \tag{14}$$

The value of $v_{3:3}^{2*}$ in (14) exceeds the intended capacity limit $p_{3:3}^*$, violating its definition.

Similarly, we regard the common highest temporal resolution of the two decision variable series as necessary to avoid the violation. When we create the constraints with the resolution in Fig. 3a, they become

$$v_{1:1}^{1*} + v_{1:2}^{2*} \le p_{1:1}^* \quad \left(c_{1:1}^{\mathrm{H}}\right) \tag{15}$$
$$v_{2:4}^{1*} + v_{1:2}^{2*} \le p_{2:2}^* \quad \left(c_{2:2}^{\mathrm{H}}\right) \tag{16}$$
$$v_{2:4}^{1*} + v_{3:3}^{2*} \le p_{3:3}^* \quad \left(c_{3:3}^{\mathrm{H}}\right) \tag{17}$$
$$v_{2:4}^{1*} + v_{4:7}^{2*} \le p_{4:4}^* \quad \left(c_{4:4}^{\mathrm{H}}\right) \tag{18}$$
$$v_{5:6}^{1*} + v_{4:7}^{2*} \le \begin{cases} \mathrm{mean}\left(p_{5:5}^*, p_{6:6}^*\right) \\ \max\left(p_{5:5}^*, p_{6:6}^*\right) \\ \min\left(p_{5:5}^*, p_{6:6}^*\right) \end{cases} \quad \left(c_{5:6}^{\mathrm{H}}\right) \tag{19}$$

Now at any time, the total output cannot exceed the capacity limit. In the case where the resolution of the capacity limit parameter is higher than that of the constraint, pre-processing is needed: In (19), we give an example of using the mean, maximum, or minimum of the parameters. The most suitable choice is contingent upon the characteristics of the specific case study and should be a calibration action of the user. In the remainder of this paper, we will present the parameters as already pre-processed to fit the temporal resolution of the constraint.

#### 2.2.3. Energy balance of conversion technologies

So far we have shown how the common highest temporal resolution is required to correctly represent instantaneous energy balances and capacity constraints. However, other types of constraints can be distorted if we use the common highest temporal resolution. For instance, consider an energy balance for a conversion technology, where, e.g., $v^{1*}$ is the non-negative energy output flow rate, and $v^{2*}$ is the non-negative energy input flow rate. Let us look at the first 3 h, disregarding the parameter $p^*$, and using the common highest temporal resolution of the decision variable series, as in Fig. 3a. Without energy losses, the energy balance of the conversion technology is

$$v_{1:1}^{1*} - v_{1:2}^{2*} = 0 \quad \left(c_{1:1}^*\right) \tag{20}$$
$$v_{2:4}^{1*} - v_{1:2}^{2*} = 0 \quad \left(c_{2:2}^*\right) \tag{21}$$
$$v_{2:4}^{1*} - v_{3:3}^{2*} = 0 \quad \left(c_{3:3}^*\right) \tag{22}$$

which can be rearranged as

$$v_{1:1}^{1*} = v_{2:4}^{1*} = v_{1:2}^{2*} = v_{3:3}^{2*} \tag{23}$$

resulting in a 3-h resolution for the variables, and therefore contradicting the intended variability of the operation.

In this case, we should use the common lowest temporal resolution of the involved variables to guarantee the intended variability of the decision variables. Algorithm 2 later shows how to obtain the lowest resolution from the involved decision variables for a constraint. Although there are different possibilities, we propose to use a "greedy" algorithm by setting time blocks of the constraint series to the latest-ending time block of the involved decision variable series. An example is given in Fig. 3b. For the first two decision variables $v_{1:1}^{1*}$ and $v_{1:2}^{2*}$, the further ending time is at the end of hour 2. Thus, the first time block of the constraint spans 2 h, giving the constraint $c_{1:2}^L$. The superscript $L$ denotes that the constraint is in the lowest temporal resolution. Subsequently, one of the decision variables $v_{2:4}^{1*}$ and $v_{3:3}^{2*}$ last until the end of the hour 4. Hence we have the constraint $c_{3:4}^{\mathrm{L}}$. Repeatedly, among $v_{5:6}^{1*}$ and $v_{4:7}^{2*}$, we have the further ending time at hour 7, therefore creating the constraint $c_{5:7}^{\mathrm{L}}$, so on and so forth. The constraints for the first 3 h are

$$v_{1:1}^{1*} + v_{2:4}^{1*} - 2v_{1:2}^{2*} = 0 \quad \left(c_{1:2}^L\right) \tag{24}$$
$$2v_{2:4}^{1*} - v_{3:3}^{2*} - v_{4:7}^{2*} = 0 \quad \left(c_{3:4}^L\right) \tag{25}$$

therefore avoiding the problem of forcing the variables to take the same value, as illustrated above in (20)–(22).

### 2.3. Algorithms to generate temporal resolutions of constraints

Here we provide the algorithms to obtain the common highest and lowest resolution of the involved decision variables for the constraints in Algorithms 1 and 2. For both algorithms, the user must provide the following information:

1. Time horizon $T \in \mathbb{Z}$, in amount of the unit time period $u$,
2. Index of the constraint $c \in \mathbb{Z}$
3. Set of decision variable indices involved in the constraint $c$: $v \in V(c) \subset \mathbb{Z}$
4. Resolutions of each decision variable, containing time blocks with starting and ending times $b_i^v = (s_i^v, e_i^v)$, where $s_i^v \le e_i^v\ \forall i \in \{1, 2, \dots, |\mathcal{R}_v|\}$.

We define each series of time blocks as a resolution $\mathcal{R}_v = \{b_1^v, b_2^v, \dots, b_{|\mathcal{R}_v|}^v\}$. The resolution fully covers the horizon with no overlap. This means that the first block in a series starts at unit period 1, $s_1^v = 1$. And the time blocks tightly follow the previous one $s_{i+1}^v = e_i^v + 1$ for $i = 1, 2, \dots, |\mathcal{R}_v| - 1$. Also, the last time block ends with the horizon $e_{|\mathcal{P}_v|}^v = T\ \forall v$. Algorithm 1 produces the common highest temporal resolution based on the involved decision variables in a constraint. This is guaranteed because every time block of the constraint ends at the nearest ending time of the time blocks of the decision variables that cover its starting time. The resulting time blocks of the constraint coincide uniquely with a time block of each involved decision variable.

**Algorithm 3** Calculating the duration of involved decision variables in a constraint.

**Input:** Resolution of the constraint $\mathcal{R}_c$
**Input:** Resolution of involved decision variables $\mathcal{R}_v,\ v \in V(c)$
**Output:** Map of duration between the decision variables and the constraint $\ell_{j,i}^{c,v}$

1: For each time block, we define a set of involved unit periods $(s : e) = \{s, s+1, \dots, e\} \subset \mathbb{Z}$
2: **for** $v \in V(c)$ **do**
3: **for** $i \in \{1, 2, \dots, |\mathcal{R}_v|\}, j \in \{1, 2, \dots, |\mathcal{R}_c|\}$ **do**
4: $\ell_{j,i}^{c,v} \leftarrow |(s_i^v : e_i^v) \cap (s_j^c : e_j^c)|$
5: **end for**
6: **end for**

Whereas in Algorithm 2, to obtain the lowest temporal resolution, every time block of the constraint lasts till the furthest ending time of the decision variable time blocks containing its starting time. Therefore, the constraint's time blocks can overlap with multiple time blocks of each involved decision variable.

The list of time blocks provided by Algorithms 1 or 2 will still be a resolution. It starts from one, according to line 2 in the two algorithms, $s_1^c = 1$. The time blocks are consecutive $s_{i+1}^c = e_i^c + 1$ for $i = 1, 2, \dots, I(c) - 1$, guaranteed by line 10. The last block ends with the horizon, $e_{|\mathcal{R}_c|}^c = T\ \forall c$ owing to the condition at line 3 in both algorithms and the fact that we require resolutions of the decision variables from the input.

### 2.4. Mapping decision variables to constraints

From the resolutions of decision variables and constraints, we need to derive the information of the duration that each decision variable is involved in the constraints. Algorithm 3 explains the details. The duration of an involved decision variable in a constraint is simply the length of the intersection of their time blocks, expressed in the number of unit periods.

## 3. Energy system optimization with fully flexible temporal resolution

In order to implement the concept of fully flexible temporal resolution, we present in this section a reformulation of an energy system optimization problem. This optimization problem has been constructed in the Tulipa Energy Model [1]. The physical characteristics we consider here are commonly used in ESOMs. Other time-coupled characteristics can also be adjusted following a similar logic (see Section 2.3).

The energy system optimization problem consists of energy assets, arranged in a set $a \in \mathcal{A}$, which includes energy producers $\mathcal{A}^{\text{producer}}$, such as renewable and conventional generation units, consumers $\mathcal{A}^{\text{consumer}}$, conversion technologies $\mathcal{A}^{\text{conversion}}$ and storage technologies $\mathcal{A}^{\text{storage}}$, like electrical batteries and pump-hydro storage. Energy exchanges between pairs of the assets are explicitly denoted with energy flow connections in a set $f \in \mathcal{F}$. Fig. 4 presents a simple example of flow connections between two zones and three assets per zone (producer, storage, and consumer). The flows are directed from an asset to another, such as electricity transmission lines and gas pipelines. Hence, each asset has a set of incoming flow connections $\mathcal{F}_a^{\text{in}}$ and outgoing flow connections $\mathcal{F}_a^{\text{out}}$. For each energy flow connection, we define a decision variable series $v_{f,i}^{\text{flow}}$, which represents the energy flow rate (e.g., in MW) of an energy carrier, for instance, natural gas, hydrogen, and electricity. Note that in the subscript, $i$ is the index of time blocks specific to this decision variable series. We assume that the parameters fit the temporal resolution of the constraints, as discussed earlier in Section 2.2. Further details of the ESOM will be provided in the following sections.

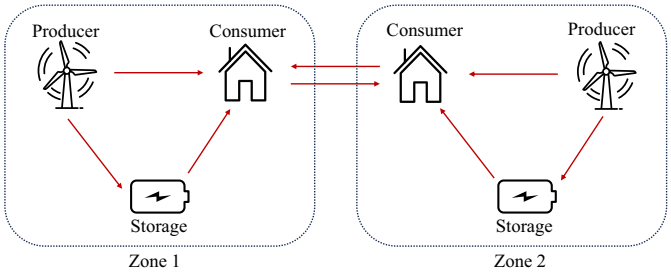


**Fig. 4.** Example of our ESOM formulation, where directed energy flow connections between pairs of the assets are modeled explicitly (arrows in red).

### 3.1. Objective function

The objective function we consider for the energy system optimization is to minimize the total investment and operational cost of the system for a "design year", given by

$$\min \left( C^{\text{invest\_asset}} + C^{\text{invest\_flow}} + C^{\text{variable\_flow}} \right) \tag{26}$$

The asset investment cost is calculated as

$$C^{\text{invest\_asset}} = \sum_{a \in \mathcal{A}} p_a^{\text{invest\_cost}} v_a^{\text{invest}} \tag{27}$$

where $p_a^{\text{invest\_cost}}$ is the asset investment cost parameter, and $v_a^{\text{invest}}$ the asset investment decision variable. Furthermore, the flow connection investment cost is given by

$$C^{\text{invest\_flow}} = \sum_{f \in \mathcal{F}} p_f^{\text{invest\_cost}} v_f^{\text{invest}} \tag{28}$$

where $\mathcal{F}$ is the set of flow connections. $p_f^{\text{invest\_cost}}$ is the flow connection investment cost parameter, and $v_f^{\text{invest}}$ the per unit investment of the flow connection. Lastly, the total variable cost of the flow connections is

$$C^{\text{variable\_flow}} = \sum_{f \in \mathcal{F}} \sum_{i=1}^{|\mathcal{R}_f|} p_f^{\text{variable\_cost}} \ell_i^f v_{f,i}^{\text{flow}} \tag{29}$$

where $|\mathcal{R}_f|$ is the number of time blocks in the resolution of the flow rate decision variable $v_{f,i}^{\text{flow}}$, $p_f^{\text{variable\_cost}}$ is the variable cost parameter per unit energy content. The energy content is the duration length $\ell_i^f$ timed by the energy flow rate $v_{f,i}^{\text{flow}}$. The duration length $\ell_i^f$ is computed as

$$\ell_i^f = e_i^f - s_i^f + 1 \quad \forall i \in \{1, 2, \dots, |\mathcal{R}_f|\} \tag{30}$$

where $e_i^f$ and $s_i^f$ are the starting and ending times of time blocks in the resolution $\mathcal{R}_f$, respectively.

### 3.2. Potential limits on investment

The capacity investments in assets and flows are bounded by their potential limits,

$$0 \le v_a^{\text{invest}} \le p_a^{\text{invest\_limit}} \quad \forall a \in \mathcal{A} \tag{31}$$

$$0 \le v_f^{\text{invest}} \le p_f^{\text{invest\_limit}} \quad \forall f \in \mathcal{F} \tag{32}$$

where $p_a^{\text{invest\_limit}}$ and $p_f^{\text{invest\_limit}}$ are investment potentials of assets and flows, respectively.

### 3.3. Capacity constraints

For each flow connection, its energy flow rate is limited by the capacity

$$0 \le v_{f,i}^{\text{flow}} \le p_f^{\text{init\_capacity}} + v_f^{\text{invest}} \quad \forall f \in \mathcal{F}, \quad \forall i \in \{1, 2, \dots, |\mathcal{R}_f|\} \tag{33}$$

where $p_f^{\text{init\_capacity}}$ is the initial capacity of the flow connection and $|\mathcal{R}_f|$ is the number of time blocks in the resolution of the flow rate decision

variable. Here, the constraint takes the decision variable's temporal resolution to ensure that every flow rate decision variable stays within its limit, as also discussed above.

The output capacity limit of a producer, conversion, or storage energy asset is exerted on the sum of the flow rates of its output flow connections, given by

$$\sum_{f\in\mathcal{F}_a^{\text{out}}}\sum_{i|\ell_{j,i}^{\text{output},a,f}>0} v_{f,i}^{\text{flow}} \le p_{a,j}^{\text{availability\_profile}}\left(p^{\text{init\_capacity}} + v_a^{\text{investment}}\right)$$
$$\forall a\in\mathcal{A}^{\text{producer}}\cup\mathcal{A}^{\text{conversion}}\cup\mathcal{A}^{\text{storage}}, \forall j\in\left\{1,2,\dots,|\mathcal{R}_a^{\text{output}}|\right\} \quad (34)$$

where $\mathcal{F}_a^{\text{out}}\subseteq\mathcal{F}$ is the set of flow connections starting from the asset and $\ell_{j,i}^{\text{output},a,f}$ is the duration of each flow decision variable in each output capacity constraint, calculated using Algorithm 3. $\ell_{j,i}^{\text{output},a,f}$ functions here as a map, hence the summation only involves the corresponding flow variables in each constraint. $p_{a,j}^{\text{availability\_profile}}$ is the availability parameter of the asset sampled in the same temporal resolution as the constraint. $p_a^{\text{init\_capacity}}$ is the initial capacity of the asset. $\mathcal{A}^{\text{producer}}$,$\mathcal{A}^{\text{conversion}}$ and $\mathcal{A}^{\text{storage}}$ are the sets of producer, conversion and storage assets, respectively. $|\mathcal{R}_a^{\text{output}}|$ is the number of time blocks in the resolution of the capacity constraint for the asset, which takes the common highest resolution of the output flow variables, described in Algorithm 1. As a result, each constraint involves each flow rate variable of a single time block.

For storage assets, the sum of the flow rates of their input flow connections is also limited by the capacity.

$$\sum_{f\in\mathcal{F}_a^{\text{in}}}\sum_{i|\ell_{j,i}^{\text{input},a,f}>0} v_{f,i}^{\text{flow}} \le p_{a,j}^{\text{availability\_profile}}\left(p_a^{\text{init\_capacity}} + v_a^{\text{investment}}\right)$$
$$\forall a\in\mathcal{A}^{\text{storage}}, \forall j\in\left\{1,2,\dots,|\mathcal{R}_a^{\text{input}}|\right\} \quad (35)$$

where $\mathcal{F}_a^{\text{in}}$ is the set of flow connections arriving at the asset and $\ell^{\text{input},a,f}$ is the duration of each flow decision variable in each input capacity constraint, calculated using Algorithm 3. The resolution $\mathcal{R}^{\text{input}}$ of the input capacity constraint uses the common highest resolution of the input flow variables.

Furthermore, the stored energy of storage assets cannot exceed the storage volume,

$$v_{ai}^{\text{stored}} \le p_a^{\text{energy\_to\_power\_ratio}}(p_a^{\text{init\_capacity}} + v_a^{\text{investment}})$$
$$\forall a\in\mathcal{A}^{\text{storage}}, \forall i\in\left\{1,2,\dots,|\mathcal{R}_a^{\text{storage}}|\right\} \quad (36)$$

where $p_a^{\text{energy\_to\_power\_ratio}}$ is the ratio between the energy storage volume and the capacity of the storage asset. In this capacity constraint, $v_{ai}^{\text{storage}}$ is the only time-coupled decision variable series. Therefore, the constraint takes the same resolution $\mathcal{R}_a^{\text{storage}}$, sharing the time blocks. The determination of this resolution will be discussed in the next section, together with the energy balance of the storage assets.

### 3.4. Instantaneous energy balances

In our formulation, instantaneous energy balances are held at the consumer assets, the energy demand needs to be satisfied by the net inflow.

$$\sum_{f\in\mathcal{F}_a^{\text{in}}}\sum_{i|\ell_{j,i}^{\text{consumer},a,f}>0} v_{f,i}^{\text{flow}} - \sum_{f\in\mathcal{F}_a^{\text{out}}}\sum_{i|\ell_{j,i}^{\text{consumer},a,f}>0} v_{f,i}^{\text{flow}} = p_{a,j}^{\text{demand\_profile}}$$
$$\forall a\in\mathcal{A}^{\text{consumer}}, \forall j\in\left\{1,2,\dots,|\mathcal{R}_a^{\text{consumer}}|\right\} \quad (37)$$

where $\ell_{j,i}^{\text{consumer},a,f}$ is the duration of each flow decision variable in each consumer balance constraint, whose resolution $\mathcal{R}_a^{\text{consumer}}$ is given by the common highest temporal resolution of input and output flows. As a result, the durations of all involved decision variables, if greater than zero, are the same. Therefore, we do not multiply the duration by the flow rate in this energy balance but assume that the demand profile $p_{a,j}^{\text{demand\_profile}}$ takes the duration into account when being sampled to the resolution of the constraint, e.g., taking the mean over the duration following (12).

### 3.5. Cumulative energy balances

As for conversion technology assets, we balance between the input and output energy contents, which are the flow rate multiplied by the duration. We also take into account the efficiency (or conversion factor):

$$\sum_{f\in\mathcal{F}_a^{\text{in}}}\sum_{i|\ell_{j,i}^{\text{conversion},a,f}>0} p_f^{\text{efficiency}}\ell_{j,i}^{\text{conversion},a,f}v_{f,i}^{\text{flow}}$$
$$= \sum_{f\in\mathcal{F}_a^{\text{out}}}\sum_{i|\ell_{j,i}^{\text{conversion},a,f}>0}\frac{1}{p_f^{\text{efficiency}}}\ell_{j,i}^{\text{conversion},a,f}v_{f,i}^{\text{flow}}$$
$$\forall a\in\mathcal{A}^{\text{conversion}}, \forall j\in\left\{1,2,\dots,|\mathcal{R}_a^{\text{conversion}}|\right\} \quad (38)$$

where $p_f^{\text{efficiency}}$ is the efficiency of the flow and $\ell_{j,i}^{\text{conversion},a,f}$ is the duration of each flow rate decision variable in each conversion balance constraint. As explained earlier in Section 2.2.3, the resolution of conversion technology assets is $\mathcal{R}_a^{\text{conversion}}$ is given by the common lowest temporal resolution using Algorithm 2.

In the storage assets, the energy balance takes into account the stored energy content every two consecutive time blocks. Therefore, the stored energy decision variable shares the same resolution as the storage energy balance:

$$v_{a,j}^{\text{stored}} = v_{a,j-1}^{\text{stored}} + v_{a,j}^{\text{inflow}} + \sum_{f\in\mathcal{F}_a^{\text{in}}}\sum_{i|\ell_{j,i}^{\text{stored},a,f}>0}\ell_{j,i}^{\text{stored},a,f}p_f^{\text{efficiency}}v_{f,i}^{\text{flow}}$$
$$- \sum_{f\in\mathcal{F}_a^{\text{out}}}\sum_{i|\ell_{j,i}^{\text{stored},a,f}>0}\frac{\ell_{j,i}^{\text{stored},a,f}v_{f,i}^{\text{flow}}}{p_f^{\text{efficiency}}}$$
$$\forall a\in\mathcal{A}^{\text{storage}}, \forall j\in\left\{1,2,\dots,|\mathcal{R}_a^{\text{stored}}|\right\} \quad (39)$$

where $v_{a,i}^{\text{inflow}}$ is a decision variable of extra energy inflow to the storage asset (for example, water flowing into a hydro reservoir) and $l_{j,i}^{\text{stored},a,f}$ is the duration of each flow decision variable in each storage balance constraint. We allow discharging the extra energy inflow, e.g., by releasing water from upstream to avoid spillage in a hydro reservoir, therefore using a decision variable and, later on an inequality constraint. The resolution $\mathcal{R}_a^{\text{stored}}$ is supposed to take the common highest temporal resolution of the input and output flow connections because the stored energy is affected by them. However, for certain storage technologies that are not sensitive to short-term variations in the stored energy, the resolution $\mathcal{R}^{\text{stored}}$ can be lower.

The extra energy inflow decision variable is bounded by the available extra energy inflow parameter:

$$v_{a,i}^{\text{inflow}} \le p_i^{\text{inflow},a} \quad \forall a\in\mathcal{A}^{\text{storage}}, \forall i\in\left\{1,2,\dots,|\mathcal{R}_a^{\text{stored}}|\right\} \quad (40)$$

In summary, and as listed in Table 1, with the proposed flexible temporal resolution formulation, the user can decide on the temporal resolutions of every energy flow and, when necessary, lower the temporal resolution of the stored energy for the storage assets. Whereas temporal resolutions of the input and output capacity constraints, as well as the consumer and conversion balance constraints are decided from other user-defined resolutions. The user can make the decisions based on the requirements of the optimization problem at hand.

### 3.6. Implementation to multi-national energy system

For a multi-national energy system, we summarize the implementation of ESOM formulation described in the previous subsections in Table 2. For energy carriers with cross-border flow connections, we create a centralized *supply hub* that receives from all producers of the given

**Table 1**
Summary of temporal resolutions and their determination.

| Temporal resolution | Equations | Determination | Requirement |
|---|---|---|---|
| Energy flow $\mathcal{R}_f^{\text{flow}}$ | (29) (30) | user-defined | None |
| Stored energy $\mathcal{R}_a^{\text{stored}}$ | (36) (39) | | $\leq$ common_highest($\mathcal{F}_a^{\text{in}} \cup \mathcal{F}_a^{\text{out}}$) |
| Output capacity $\mathcal{R}_a^{\text{output}}$ | (34) | computed from other resolutions | = common_highest($\mathcal{F}_a^{\text{out}}$) |
| Input capacity $\mathcal{R}_a^{\text{input}}$ | (35) | | = common_highest($\mathcal{F}_a^{\text{in}}$) |
| Consumer balance $\mathcal{R}_a^{\text{consumer}}$ | (37) | | = common_highest($\mathcal{F}_a^{\text{in}} \cup \mathcal{F}_a^{\text{out}}$) |
| Conversion balance $\mathcal{R}_a^{\text{conversion}}$ | (38) | | = common_lowest($\mathcal{F}_a^{\text{in}} \cup \mathcal{F}_a^{\text{out}}$) |

**Table 2**
Summary of the asset types and flow connections between the assets of each country in the multi-national energy system.

| Problem feature | Definition in the ESOM |
|---|---|
| Consumer assets | Instantaneous energy balance including a demand profile |
| Producer assets | Produce energy from sources external to the ESOM |
| Conversion assets | Convert energy between different carriers within the ESOM |
| Storage assets | Store energy with an optional extra energy inflow |
| Flow connections (Cross-border) | Supply hub* → Neighbors' consumer<br>Neighbors' supply hub → Domestic consumer<br>Producer → Supply hub<br>Supply hub → Consumer |
| Flow connections (Domestic) | Supply hub → Storage<br>Supply hub → Conversion<br>Storage → Consumer<br>Conversion → Consumer<br>Conversion → Storage |

* Supply hub is a consumer asset with no demand for energy carriers that have cross-border flow connections, created to limit arbitrary symmetrical solutions.

**Table 3**
Summary of the assumptions for energy assets and flows considered for each country in the EU + 3 energy system optimization case study.

| Problem feature | Element | Setup |
|---|---|---|
| Consumer assets | Electricity demand | Hourly series from TYNDP |
| | Hydrogen demand | Constant hourly mean from TYNDP |
| Producer assets | Blue hydrogen import | Unlimited import at a fixed price |
| | Electricity energy not served | Unlimited cut-off with a fixed penalty |
| | Onshore wind turbines* | Greenfield investment within TYNDP capacities |
| | Offshore wind turbines* | Greenfield investment without limits |
| | Solar PV* | |
| | Run-of-river hydro | Operation with TYNDP capacities |
| | Nuclear plants | |
| Conversion assets | PEM electrolyzer | Greenfield investment without limits |
| | PEM fuel cell | |
| Storage assets | Electric battery | |
| | Hydrogen tank | |
| | Hydro reservoir | Operation with TYNDP capacities |
| | Closed pumped hydro storage | |
| | Open pumped hydro storage | |
| Flows | Electricity cross-border | |
| | Electricity domestic | Operation limited by assets' capacities |
| | Hydrogen domestic | |

* Our formulation allows output curtailments of renewable energy producer assets.

carrier. This supply hub then supplies the neighbor countries' consumer assets, as well as domestic consumer, storage, and conversion assets. This way, the domestic consumer can only be satisfied by domestic or neighbors' producers, but not from producers located further away, e.g., neighbors' neighbors. The structure is intended to limit symmetrical solutions where the location of certain producer and storage asset capacities becomes arbitrary due to the cross-border flow connections, as we also assume the same cost parameters across countries. Likewise, we designate that the conversion and storage assets are only provided to the domestic consumers.

## 4. Demonstration of the flexible temporal resolution: a european energy system case study

### 4.1. Case study EU + 3

To demonstrate the potential and benefits of the proposed fully flexible temporal resolution method, we built a case study for a future energy system in EU-27 countries plus the UK, Norway and Switzerland, abbreviated hereafter as *EU + 3*. While we don't aim at using this case study to provide any policy insight on the European energy system design and operation, we want to use a relevant exemplary case that is close in size and complexity to applications of real interest. Therefore, the case study builds upon the dataset presented in the TYNDP 2022 publication from ENTSO-E and, more specifically, the National Trends 2030 scenario using the weather year 2008 [37]. Following Table 2, we represent each country by assets and flow connections, which represent technologies and electricity grid connections listed in Table 3.

The energy system optimization problem includes both design and operation variables of different technologies and energy carriers, and further optimizes the TYNDP system layout to achieve a fossil-free system. As specified in Table 3, we remove all fossil assets while allowing for optimizing the capacity of the following technologies: (i) green hydrogen conversion technologies (fuel cells, electrolyzers); (ii) on/offshore wind turbines and solar PV; (iii) electric batteries and hydrogen storage. On the other hand, we leave the installed capacities for hydropower plants, pump hydro storage, reservoirs and nuclear power plants at the anticipated values from the National Trends scenario because in the case of hydro, the techno-economic potential in Europe has been largely exploited and further expansion is not possible without unwanted environmental impact. In the case of nuclear power plants, further expansion is uncertain because of high costs, large environmental impact and low social acceptance. Therefore, we optimize for their operation exclusively.

The case study is realized using Tulipa Energy Model version 0.7.0 [1], which implements the energy system optimization problem described in (26)–(40), including Algorithms 1–3. The optimization problems are solved using Gurobi 12 [38], on a personal computer with a CPU of Intel i9-13900H 2.60 GHz, and 32 GB of RAM. The input data files are available in [39].

### 4.2. Benchmarking

To investigate the impact on the computational performance and the quality of the solution, we consider as accuracy benchmark the EU + 3

case study solved with hourly resolution for a 1-year horizon, i.e., 8760 consecutive hours, as provided in the input hourly series (hereafter *UTR-1h*, or *Uniform Time Resolution-1 hour*). On the other side of the spectrum, we consider cases with aggregated consecutive hours as the simplest approach to reduce computational complexity arising from the time discretization. We therefore solve the system by aggregating hourly values to 2-h, 3-h, 4-h, and 5-h (hereafter referred to as *UTR-2h*, *UTR-3h*, *UTR-4h*, and *UTR-5h*, respectively). The distribution of time blocks in these configurations is illustrated in Fig. 6.

We benchmark the fully flexible temporal resolution formulation against these cases by implementing two different configurations. These are two exemplary cases of how the temporal flexibility could be exploited in practice, but we note that many more configurations can be designed when making use of this new flexibility feature.

- The first flexible temporal resolution configuration is named *Flexible Temporal Resolution Nightveil* (*FTR-NV*), where we aggregate the output flow rate decision variables of solar photovoltaic (PV) units during the nights when their availability is continuously zero for each of the 30 countries, as illustrated in Fig. 6. As an example, for the Netherlands, we reduce the number of decision variables in solar PV from 8760 to 4683. The goal of this configuration is to show that the flexible temporal resolution allows for removal of unnecessary variables, where these variables have a non-trivial sequencing in time along the year. Therefore, the solution has the same quality as the benchmark 1-h case, with no additional computation time (possibly a faster solution by having a smaller problem).
- The second flexible temporal resolution configuration implements a geographically decreasing temporal resolution, which is associated with the degree of connection (DoC) to the target country, in our case, the Netherlands (NL), as shown in Figs. 5 and 6. The temporal resolutions are set at the country level, which decides the user-defined resolutions in Table 1. Different from FTR-NV, the duration of time blocks is constant across the horizon, except for the last one if the horizon cannot be divided exactly by the duration. Transport flow connections between two countries adopt the resolution of the country with a shorter duration. The hypothesis leading to such a configuration is that by reducing the temporal resolutions gradually as we move further away from the target country, we could improve the computational performance by getting a relatively more accurate solution for the target country while the solution process requires less time. To the best of our knowledge, our formulation is the first among energy system optimization models that makes such gradual increments in duration possible. This configuration is named *Flexible Temporal Resolution Geographically Decreasing* (*FTR-GD*),

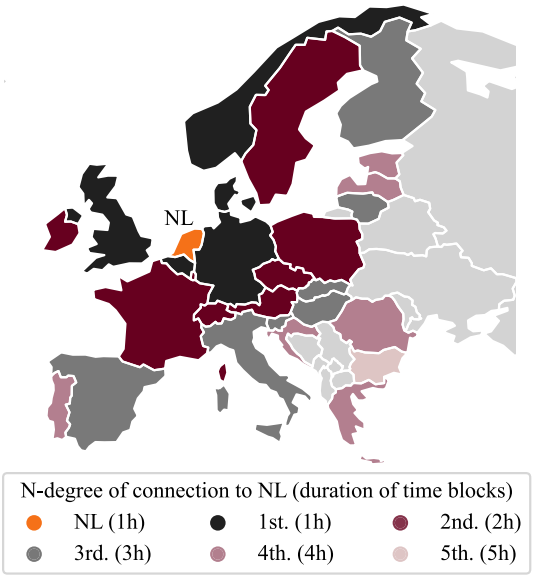


**Fig. 5.** European countries included the EU + 3 case study. The color denotes the degree of connection to the Netherlands (NL) and the duration of time blocks related to each country in geographically decreasing temporal resolution configuration (FTR-GD).

### 4.3. Feasibility test of the solution quality

Aside from comparing the system capacity design, we conduct feasibility tests on the simplified configurations (UTR-2h, UTR-3h, UTR-4h, UTR-5h, FTR-NV and FTR-GD). This is done by taking their capacity investment decisions as initial capacities, then operating the system in uniform hourly resolution (with no investable capacities). The solution quality is evaluated by comparing the resulting total energy not served in the system operation with that of the benchmark model. We expect that insufficient (often cheaper) system designs would lead to a reduced level of feasibility, which is reflected in additional energy not served in the solution of the hourly dispatch problem.

Since FTR-GD has a premise of geographical focus, we conduct the feasibility test on two geographical scales, the Netherlands and the whole EU + 3 system. In the former case, we only insert the capacity design of the Netherlands into the dispatch problem, while capacities in the other countries are taken from the benchmark model UTR-1h.

## 5. Results and discussion

After solving the optimization problems, we examine the solutions resulting from using uniform, geographically decreasing, and nightveil temporal resolutions. As shown in Table 4 and Figs. 7–9, we compare the solutions in three dimensions. The first is the wall clock time that the optimization process took, representing the computational cost. The second aspect refers to the differences in capacity design, measuring the deviation from the benchmark model (UTR-1h), where all time-dependent decision variables and constraints are in the hourly resolution. Last but not least, we assess the solutions with the feasibility test of the solution quality, as explained earlier in Section 4.3.

First, it can be noted that the objective function remains very close to reference hourly resolution for UTR-2h and FTR-GD, while it is the same for FTR-NV. For all other averaging methods, the deviation is larger: a lower total cost is found but, as we discuss later, with repercussions on the quality of the solution. When looking at the computation time, we can note a few different indications. Despite the fact that Algorithms 1, 2, and 3 conduct arithmetic computations, the total problem formulation time remains substantially similar to the reference UTR-1h, increasing by 0.3 minute in the case of FTR-GD, and decreasing by 0.1 minute for FTR-NV (it is worth noting, that the problem formulation time is less than 5 % of the total computation time). The savings in the formulation time of FTR-NV are due to the reduction of the decision variables and constraints, which can also be seen in UTR-2/3/4/5h. Moreover, it can be noted that the computation time of the solution sharply decreases when adopting FTR-GD. UTR-2/3/4/5h has lower solve time, which is however paid in lower solution quality. To better illustrate this, Fig. 7 shows the wall clock time of the solution process vs. The mean absolute error in capacity investments, for the Netherlands only (Fig. 7a) as well as for the EU + 3 (Fig. 7b); the exact numerical values are reported in Table 4. As expected, the solutions of uniform temporal resolutions (in gray in the figure) form a Pareto front, by which there is a trade-off between the accuracy of the solution and the computational cost: we pay for reduction in computational complexity with a decrease in solution accuracy.

However, this is not the case when using the flexible temporal resolution. First of all, we notice that, irrespective of focusing on the Netherlands or the EU, FTR-NV produces exactly the same solution as the benchmark. This is because in the FTR-NV, we flexibly remove the


**Fig. 6.** Distribution of time blocks (a sample day in alternating colors) for the temporal resolution adopted in the different case studies tested here. From top to bottom: UTR-1h, UTR-2h, UTR-3h, UTR-4h, UTR-5h, FTR-NV, and FTR-GD. Note that FTR-NV has varying time length of solar PV at night according to the hours of sun during an year.

**Table 4**
Key performances of the different temporal resolution configurations, including objective value, solve time, formulation time, mean absolute error (MAE) in capacity investments for the target country, the Netherlands (NL), and additional energy not served (ENS) in the entire EU + 3 system in the feasibility test on NL.

| Temporal resolution | Objective value (B€) | Wall time solve (min) | Wall time formulation (min) | MAE capacity in NL (GW) | Feasibility test on NL (Add. GWh ENS in EU + 3) |
|---|---|---|---|---|---|
| UTR-1h | 164.0 | 51.4 | 2.5 | 0.0 | 0.0 |
| UTR-2h | 163.3 | 12.7 | 1.4 | 0.44 | 62.3 |
| UTR-3h | 161.8 | 5.2 | 0.9 | 1.16 | 178.0 |
| UTR-4h | 161.6 | 2.9 | 0.8 | 1.18 | 396.9 |
| UTR-5h | 159.4 | 2.2 | 0.7 | 2.23 | 276.2 |
| FTR-NV | 164.0 | 50.8 | 2.4 | 0.0 | 0.0 |
| FTR-GD | 163.1 | 28.0 | 2.8 | 0.11 | 9.2 |

decision variables of solar PV output when not needed, i.e., when the sun availability and the PV production capacity are zero. The solution comes with barely any difference in the solve time - just slightly faster (the solver is expected to handle the decision variables that are bound to be zeros early in the solution process, therefore removing them from the set of variables). Secondly, we notice that FTR-GD allows for a significant computational speedup. Fig. 7a shows that the solution quality in the Netherlands exceeds the Pareto front when using the Dutch-centered geographically decreasing temporal resolution. Compared to the benchmark model, FTR-GD reduces the computation time by 45.4 %. Compared to the best uniform alternative UTR-2h, FTR-GD incurs about 24.3 % of the mean absolute error in system capacities, as also shown in Table 4. This improvement comes at the expense of solution quality outside of the Netherlands. When we zoom out to the whole system, in Fig. 7b, the Dutch-centered geographically decreasing temporal resolution is less appealing than the uniform group, as expected. We note, however, that this is just an illustrative application. More temporal resolution configurations enabled by the fully flexible temporal resolution formulation are to be explored.

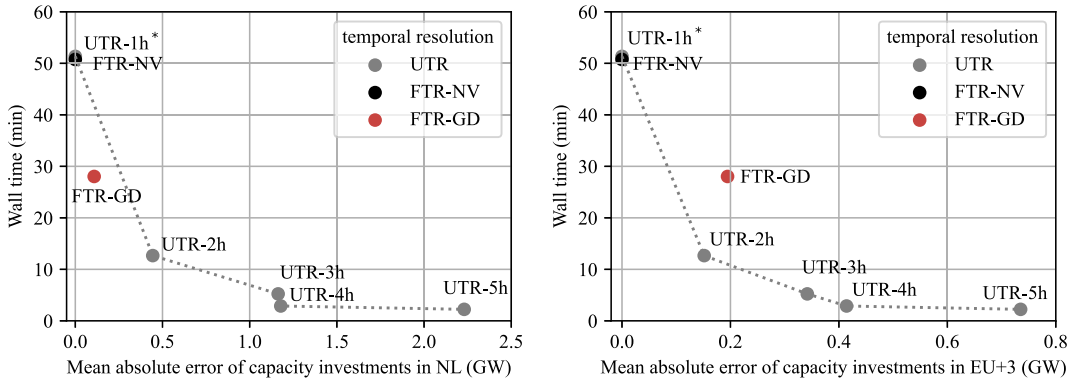


**Fig. 7.** Mean absolute error of capacity investments compared to the benchmark UTR-1h, (a) in the Netherlands and (b) in the whole EU + 3 system.

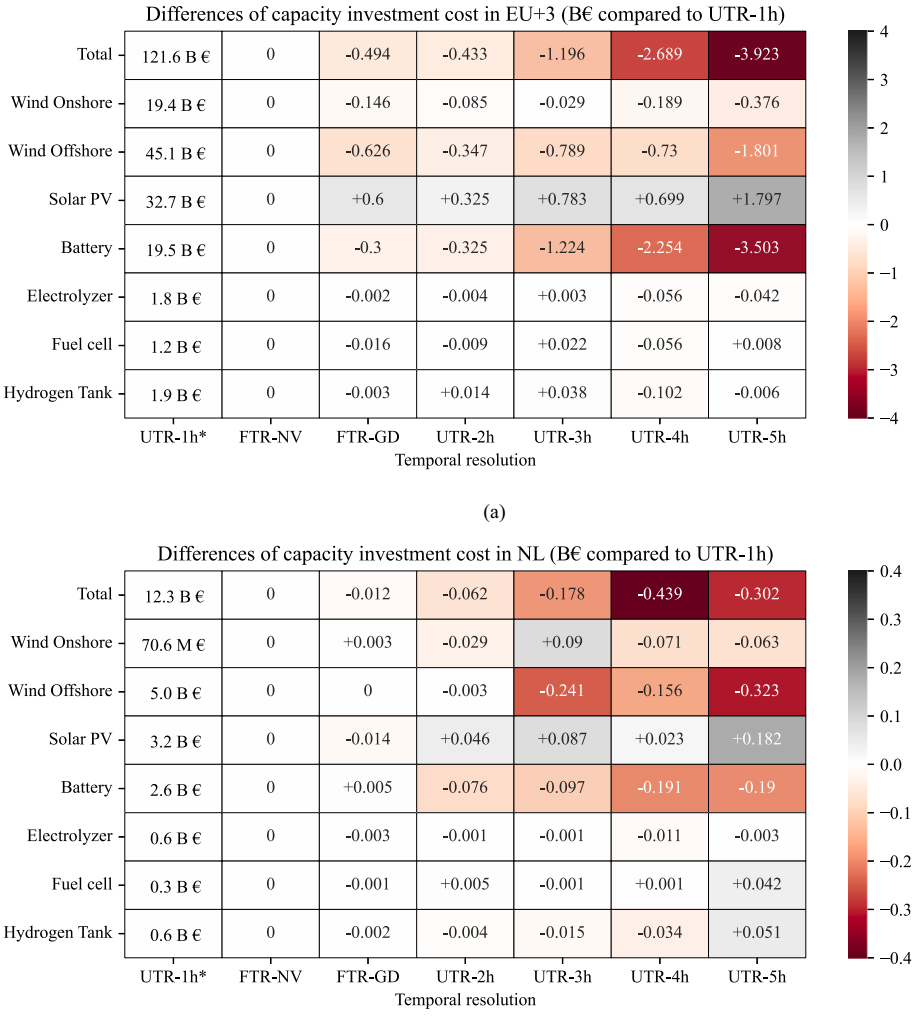


**Fig. 8.** Differences of capacity investment cost compared to the benchmark UTR-1h, (a) in the Netherlands and (b) in the whole EU + 3 system including the Netherlands.

To examine the results more thoroughly, Fig. 8 presents the detailed differences in capacity investment costs for the Netherlands and the entire EU + 3 system. In Fig. 8a, the total capacity investment cost in EU + 3 consistently decreases from UTR-2h to UTR-5h in the uniform resolution group, demonstrating a growing underestimation of the capacity requirements as the temporal details of the system diminish. Similarly, in Fig. 8b, the reduction in total capacity investment occurs for the Netherlands, up to UTR-4h. When the (uniform) temporal resolution is further aggregated from 4-h to 5-h, the total investment cost in the Netherlands increases – showing a shift in capacity investment from other countries to the Netherlands. This can be attributed to the temporal idiosyncrasy of each country within the interconnected EU + 3 system. Consequently, the relative distribution of capacity investments changes depending on the temporal resolution configurations, even with uniform aggregations.

Compared with the UTR group, both FTR-NV and FTR-GD stand out in terms of the accuracy of capacity investment estimates, reinforcing the results shown earlier in Fig. 8. The FTR-NV, with redundant decision variables removed, produces a solution identical to the benchmark UTR-1h. For the Netherlands, the target country of FTR-GD, it yields a significantly more accurate solution than any of the UTR configurations, particularly in the electricity sector.

It is worth noting that optimal investment decisions in different technologies have different sensitivities to the temporal resolution. This is particularly the case for renewable energy technologies and batteries, as they are highly sensitive to the temporal resolution of the model. As shown in Fig. 8a for both FTR-GD and the UTR group, investment in solar PV increases whenever temporal aggregation is applied during daylight hours. This outcome is intuitive: when the availability of solar PV output is artificially spread from the noon peak into adjacent morning and afternoon hours, or even extended erroneously into nighttime hours (e.g. for UTR-5h), solar PV becomes much more capable of flexibly satisfying the demand, owing to the longer operable periods and less fluctuating availability, together with the curtailment option. As a result, investments in wind turbines and battery storage decrease in the optimal system design. It is worth noting that the flexible time resolution method allows for modeling all undispatchable renewable-based technologies with hourly resolution, while having other generators with multi-hour resolution.

When analyzing battery storage, it can be noted that it is gradually less required in the optimal system design when the temporal resolution decreases, both in the Netherlands and in the whole system. As the periods are aggregated, the temporal mismatch between the energy demand and the availability of variable renewable production flattens out. The monotonic decrease tells the positive relation between electricity storage and temporal resolution.

However, the deviations in the capacity investment brought by progressively coarser uniform temporal aggregation are not necessarily monotonic. For instance, the capacity investment cost on onshore wind turbines in Fig. 8a reduces by 85.4 M€under UTR-2h, but only 28.7 M€under UTR-3h, then further reduced in the cases of UTR-4h and UTR-5h. Such inhomogeneous deviations stem from the temporal rematching under the changing temporal resolutions, where different hours are associated with each other, leading to investment patterns that cannot be simply interpolated in a top-down manner. This effect is even more pronounced when we zoom in on individual countries.

The hydrogen sector is less susceptible to the impact of temporal details. One contributing reason is that we have assumed, over the horizon, a constant hydrogen demand. Hence, the hydrogen tank storage is driven only by the long-term variation in the supply. Additionally, the energy system is dominated by the electricity sector, which further reduces the relative impact on hydrogen-related investments. Therefore, the changes with different temporal resolutions do not significantly affect the total investments in hydrogen. Nevertheless, the general trend of reduced capacity requirements and the inhomogeneous deviations resulting from the temporal aggregations are also present in the hydrogen sector, as shown in both Fig. 8a and b.

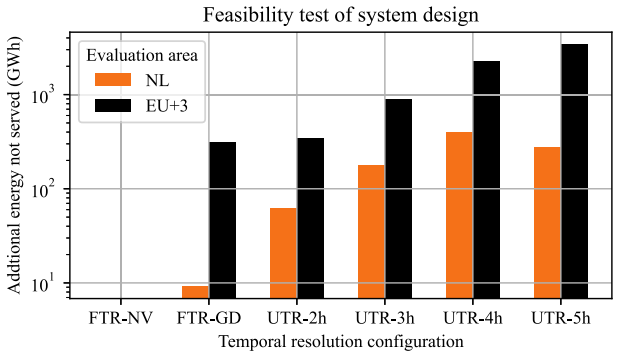


**Fig. 9.** Additional energy not served in the feasibility test of system design resulting from the UTR and FTR temporal resolutions, compared to the benchmark UTR-1h. Note that FTR-NV does not introduce any additional energy-not-served, for either NL or the rest of the EU + 3.

The additional energy not served in the optimal operation test is plotted in Fig. 9 and confirms that: (i) FTR-NV reproduces the exact solution as UTR-1h; (ii) the geographically decreasing temporal resolution leads to a better solution quality in the Netherlands than the uniform group. Specifically, the geographically decreasing temporal resolution avoids 85 % of the additional energy not served when compared with UTR-2h, the best uniform alternative, as also provided in Table 4. The solution quality of the whole EU + 3 system is similar for FTR-GD and UTR-2h, while it deteriorates sharply when increasing the uniform time aggregation. The energy not served for the Netherlands follows a similar pattern, but with a better solution quality when the problem is formulated in 5 h than in 4 h uniform temporal resolution. This is somewhat counterintuitive, but can be explained by the higher capacity investments in the Netherlands, especially in the solar PV and the hydrogen sector, as shown in Fig. 8b.

## 6. Conclusion

In this paper, we proposed the concept of fully flexible temporal resolution for energy system optimization models. We provide a mathematical formulation that allows each decision variable and constraint to have a separate temporal resolution that can also vary dynamically across the time horizon. In order to guarantee that the physical laws embedded in the classical formulation are respected (e.g., capacity limits, energy balances), we take special care in reconciling constraints with the time series of the decision variables. Accordingly, we create the algorithms needed to derive the common highest and common lowest temporal resolution from the resolutions of decision variables, provided by user input. Then, we calculate the durations to map the involved decision variables to the constraints. Putting the above ingredients together, we reformulated a classical energy system optimization problem with capacity investment and operation decisions, so it now allows for fully flexible temporal resolution.

To demonstrate the potential benefits of the fully flexible temporal resolution formulation, we benchmarked two possible flexible configurations against the uniform 1 h case (precise, but computationally demanding) and four additional cases with uniform multi-hour aggregation (faster, but with lower accuracy). The two flexible temporal resolution configurations included a nightveil case (no PV decision variables between sunset and sunrise) and a geographically decreasing temporal resolution in the surrounding countries based on their degree of connection to the target country, both enabled by the proposed formulation. We implemented them in a case study of the energy system of the 27 EU countries plus the UK, Norway and Switzerland (EU + 3).

Starting with TYNDP 2022 data [37], the objective of this case study is to acquire the optimal capacity investment decisions and the corresponding operation of energy conversion and storage assets, in a fully decarbonized scenario.

Results show that the model with geographically decreasing temporal resolution exceeds the Pareto front between computational cost and the solution accuracy, existing in uniform temporal resolutions. In the target country (the Netherlands in this case), the model produces a more accurate solution, which simultaneously solves faster than the uniform 1-h temporal resolution, with a 45.4 % reduction in computation time. In the solution, the model avoids large discrepancies in onshore wind turbines and battery storage, which are sensitive to the temporal resolution. It produces a solution of higher quality, having 75 % less mean absolute error in the capacity investment decisions than the best uniform alternative (UTR-2h), which results in 85.2 % lower additional energy not served in the system design feasibility test. Moreover, the flexible nightveil case yields a smaller model, producing an identical solution to the benchmark.

Such preliminary yet promising examples demonstrate that the proposed formulation of fully flexible temporal resolution opens up opportunities to enhance the computational efficiency of energy system optimization models. To this end, we encourage future studies, e.g., exploiting the power of machine learning, to leverage our formulation and explore improved combinations of temporal resolutions to maximize the benefits.

## CRediT authorship contribution statement

**Zhi Gao:** Conceptualization, Writing – original draft, Visualization, Validation, Methodology, Investigation, Formal analysis, Data curation. **Matteo Gazzani:** Conceptualization, Writing – review & editing, Validation, Supervision, Funding acquisition. **Diego A. Tejada-Arango:** Writing – review & editing, Software, Methodology, Data curation. **Abel Soares Siqueira:** Writing – review & editing, Software, Methodology. **Ni Wang:** Writing – review & editing, Software, Methodology. **Madeleine Gibescu:** Writing – review & editing, Supervision, Funding acquisition. **Germán Morales-España:** Writing – review & editing, Methodology, Supervision, Validation, Funding acquisition.

## Declaration of generative AI and AI-assisted technologies in the writing process

During the preparation of this work, the author(s) used ChatGPT in order to proofread the manuscript. After using this tool/service, the author(s) reviewed and edited the content as needed and take(s) full responsibility for the content of the publication.

## Declaration of competing interest

The authors declare that they have no known competing financial interests or personal relationships that could have appeared to influence the work reported in this paper.

## Acknowledgements

This publication is part of the project NextGenOpt with project number ESI.2019.008, which is (partly) financed by the Dutch Research Council (NWO) and supported by eScienceCenter under project number NLeSC C 21.0226. In addition, this research received partial funding from the European Climate, Infrastructure and Environment Executive Agency under the European Union's HORIZON Research and Innovation Actions under grant agreement no. 101095998.

## Data availability

Data and codes are available, links provided in the manuscript.

## References

[1] Siqueira AS, Tejada-Arango DA, Morales-España G, Neustroev G, Kiviluoma J, Clisby L, et al. Tulipa energy model; 2024. https://github.com/TulipaEnergy/TulipaEnergyModel.jl
[2] International Energy Agency. Net zero by 2050; 2021. https://www.iea.org/reports/net-zero-by-2050
[3] Intergovernmental Panel on Climate Change. Synthesis report. Contribution of working groups I, II and III to the sixth assessment report of the intergovernmental panel on climate change. Clim Change 2023:35–115. https://doi.org/10.59327/IPCC/AR6-9789291691647. https://www.ipcc.ch/report/ar6/syr/
[4] Kotzur L, Nolting L, Hoffmann M, Groß T, Smolenko A, Priesmann J, et al. A modeler's guide to handle complexity in energy systems optimization. Adv Appl Energy 2021;4:100063. https://doi.org/10.1016/j.adapen.2021.100063. https://www.sciencedirect.com/science/article/pii/S266679242100055X
[5] DeCarolis J, Daly H, Dodds P, Keppo I, Li F, McDowall W, et al. Formalizing best practice for energy system optimization modelling. Appl Energy 2017;194:184–98. https://doi.org/10.1016/j.apenergy.2017.03.001. https://www.sciencedirect.com/science/article/pii/S0306261917302192
[6] Fattahi A, Sánchez Diéguez M, Sijm J, España GM, Faaij A. Measuring accuracy and computational capacity trade-offs in an hourly integrated energy system model. Adv Appl Energy 2021;1:100009. https://doi.org/10.1016/j.adapen.2021.100009. https://www.sciencedirect.com/science/article/pii/S2666792421000020
[7] Wuijts R, Akker J, Broek M. Effect of modelling choices in the unit commitment problem. Energy Syst 2023 https://doi.org/10.1007/s12667-023-00564-5.
[8] Helistö N, Kiviluoma J, Morales-España G, O'Dwyer C. Impact of operational details and temporal representations on investment planning in energy systems dominated by wind and solar. Appl Energy 2021;290:116712. https://doi.org/10.1016/j.apenergy.2021.116712. https://www.sciencedirect.com/science/article/pii/S0306261921002312
[9] European Network of Transmission System Operators for Electricity. Vision on market design and system operation towards 2030; 2019. https://www.entsoe.eu/publications/
[10] Mohammadi M, Noorollahi Y, Mohammadi-Ivatloo B, Yousefi H. Energy hub: from a model to a concept – a review. Renew Sustain Energy Rev 2017;80:1512–27. https://doi.org/10.1016/j.rser.2017.07.030. https://www.sciencedirect.com/science/article/pii/S1364032117310985
[11] Frysztacki MM, Hörsch J, Hagenmeyer V, Brown T. The strong effect of network resolution on electricity system models with high shares of wind and solar. Appl Energy 2021;291:116726. https://doi.org/10.1016/j.apenergy.2021.116726. https://www.sciencedirect.com/science/article/pii/S0306261921002439
[12] Hofmann F, Tries C, Neumann F, Zeyen E, Brown T. $H_2$ and $CO_2$ network strategies for the European energy system. Nat Energy 2025. https://doi.org/10.1038/s41560-025-01752-6
[13] Weimann L, Gazzani M. A novel time discretization method for solving complex multi-energy system design and operation problems with high penetration of renewable energy. Comput Chem Eng 2022;163:107816. https://doi.org/10.1016/j.compchemeng.2022.107816. https://www.sciencedirect.com/science/article/pii/S0098135422001545
[14] Tejada-Arango DA, Morales-España G, Wogrin S, Centeno E. Power-based generation expansion planning for flexibility requirements. IEEE Trans Power Syst 2020;35:2012–23. https://doi.org/10.1109/TPWRS.2019.2940286
[15] Priesmann J, Nolting L, Praktiknjo A. Are complex energy system models more accurate? an intra-model comparison of power system optimization models. Appl Energy 2019;255:113783. https://doi.org/10.1016/j.apenergy.2019.113783. https://www.sciencedirect.com/science/article/pii/S0306261919314709
[16] Teichgraeber H, Brandt AR. Time-series aggregation for the optimization of energy systems: goals, challenges, approaches, and opportunities. Renew Sustain Energy Rev 2022;157:111984. https://doi.org/10.1016/j.rser.2021.111984. https://www.sciencedirect.com/science/article/pii/S1364032121012478
[17] Kotzur L, Nolting L, Hoffmann M, Groß T, Smolenko A, Priesmann J, et al. A modeler's guide to handle complexity in energy systems optimization. Adv Appl Energy 2021;4:100063. https://doi.org/10.1016/j.adapen.2021.100063. https://www.sciencedirect.com/science/article/pii/S266679242100055X
[18] Shirizadeh B, Quirion P. Do multi-sector energy system optimization models need hourly temporal resolution? A case study with an investment and dispatch model applied to france. Appl Energy 2022;305:117951. https://doi.org/10.1016/j.apenergy.2021.117951. https://www.sciencedirect.com/science/article/pii/S0306261921012617
[19] Kotzur L, Markewitz P, Robinius M, Stolten D. Impact of different time series aggregation methods on optimal energy system design. Renew Energy 2018;117:474–87. https://doi.org/10.1016/j.renene.2017.10.017. https://www.sciencedirect.com/science/article/pii/S0960148117309783
[20] Tejada-Arango DA, Domeshek M, Wogrin S, Centeno E. Enhanced representative days and system states modeling for energy storage investment analysis. IEEE Trans Power Syst 2018;33:6534–44. https://api.semanticscholar.org/CorpusID:53013208
[21] Gabrielli P, Gazzani M, Martelli E, Mazzotti M. Optimal design of multi-energy systems with seasonal storage. Appl Energy 2018;219:408–24. https://doi.org/10.1016/j.apenergy.2017.07.142. https://www.sciencedirect.com/science/article/pii/S0306261917310139
[22] Johnston J, Henriquez-Auba R, Maluenda B, Fripp M. Switch 2.0: a modern platform for planning high-renewable power systems. SoftwareX 2019;10:100251. https://doi.org/10.1016/j.softx.2019.100251. https://www.sciencedirect.com/science/article/pii/S2352711018301547
[23] PyPSA. PyPSA: Python for power system analysis; 2023. https://pypsa.readthedocs.io/en/latest/

[24] Neumann F, Hagenmeyer V, Brown T. Assessments of linear power flow and transmission loss approximations in coordinated capacity expansion problems. Appl Energy 2022;314:118859. https://doi.org/10.1016/j.apenergy.2022.118859. https://www.sciencedirect.com/science/article/pii/S0306261922002938
[25] Wiese F, Bramstoft R, Koduvere H, Alonso AP, Balyk O, Kirkerud JG, et al. Balmorel open source energy system model. Energy Strategy Rev 2018;20:26–34. https://doi.org/10.1016/j.esr.2018.01.003. https://www.sciencedirect.com/science/article/pii/S2211467X18300038
[26] TEMOA. TEMOA: tools for energy model optimization and analysis; 2023. https://temoacloud.com/
[27] Patankar N, Fell HG, Rodrigo de Queiroz A, Curtis J, DeCarolis JF. Improving the representation of energy efficiency in an energy system optimization model. Appl Energy 2022;306:118083. https://doi.org/10.1016/j.apenergy.2021.118083. https://www.sciencedirect.com/science/article/pii/S0306261921013696
[28] Ihlemann M, Kouveliotis-Lysikatos I, Huang J, Dillon J, O'Dwyer C, Rasku T, et al. Spineopt: a flexible open-source energy system modelling framework. Energy Strategy Rev 2022;43:100902. https://doi.org/10.1016/j.esr.2022.100902. https://www.sciencedirect.com/science/article/pii/S2211467X22000955
[29] Renaldi R, Friedrich D. Multiple time grids in operational optimisation of energy systems with short- and long-term thermal energy storage. Energy 2017;133:784–95. https://doi.org/10.1016/j.energy.2017.05.120. https://www.sciencedirect.com/science/article/pii/S0360544217308782
[30] Zhou Y, Min C, Wang K, Xie L, Fan Y. Optimization of integrated energy systems considering seasonal thermal energy storage. J Energy Storage 2023;71:108094. https://doi.org/10.1016/j.est.2023.108094. https://www.sciencedirect.com/science/article/pii/S2352152X23014913
[31] Brown T, Bischof-Niemz T, Blok K, Breyer C, Lund H, Mathiesen B. Response to 'burden of proof: a comprehensive review of the feasibility of 100 % renewable-electricity systems. Renew Sustain Energy Rev 2018;92:834–47. https://doi.org/10.1016/j.rser.2018.04.113. https://www.sciencedirect.com/science/article/pii/S1364032118303307
[32] Deane J, Drayton G, Ó Gallachóir B. The impact of sub-hourly modelling in power systems with significant levels of renewable generation. Appl Energy 2014;113:152–58. https://doi.org/10.1016/j.apenergy.2013.07.027. https://www.sciencedirect.com/science/article/pii/S030626191300593X
[33] Zhang N, Jiang H, Du E, Zhuo Z, Wang P, Wang Z, et al. An efficient power system planning model considering year-round hourly operation simulation. IEEE Trans Power Syst 2022;37:4925–35. https://doi.org/10.1109/TPWRS.2022.3146299
[34] Neumann F, Zeyen E, Victoria M, Brown T. The potential role of a hydrogen network in europe. Joule 2023;7:1793–817. https://doi.org/10.1016/j.joule.2023.06.016. https://www.sciencedirect.com/science/article/pii/S2542435123002660
[35] Martínez-Gordón R, Gusatu L, Morales-España G, Sijm J, Faaij A. Benefits of an integrated power and hydrogen offshore grid in a net-zero north sea energy system. Adv Appl Energy 2022;7:100097. https://doi.org/10.1016/j.adapen.2022.100097. https://www.sciencedirect.com/science/article/pii/S2666792422000154
[36] Morales-España G, Hernández-Serna R, Tejada-Arango DA, Weeda M. Impact of large-scale hydrogen electrification and retrofitting of natural gas infrastructure on the European power system. Int J Electr Power Energy Syst 2024;155:109686. https://doi.org/10.1016/j.ijepes.2023.109686. https://www.sciencedirect.com/science/article/pii/S0142061523007433
[37] ENTSO-E. Ten-year network development plans; 2024. https://tyndp.entsoe.eu/
[38] Gurobi. Gurobi opimization; 2024. https://www.gurobi.com/
[39] Gao Z. Input data files for fully flexible temporal resolutions; 2025. https://github.com/gzclarence/Fully-Flexible-Temporal-Resolution